

# THE CAVITATION NUCLEI TRANSIENT CHARACTERISTICS OF LENNARD-JONES FLUID IN CAVITATION INCEPTION

Fu Qiang, Dr.

Zhang Benying, M.S.

Zhao Yuanyuan, Dr.

Zhu Rongsheng, Prof. Dr.

Liu Gang, M.S.

Li Mengyuan, M.S.

National Research Center of Pumps, Jiangsu University, Zhenjiang, Jiangsu, China

## ABSTRACT

*In the field of ocean engineering, cavitation is widespread, for the study of cavitation nuclei transient characteristics in cavitation inception, we applied theoretical analysis and molecular dynamics (MD) simulation to study Lennard-Jones (L-J) fluid with different initial cavitation nuclei under the NVT-constant ensemble in this manuscript. The results showed that in cavitation inception, due to the decrease of liquid local pressure, the liquid molecules would enter the cavitation nuclei, which contributed to the growth of cavitation nuclei. By using molecular potential energy, it was found that the molecular potential energy was higher in cavitation nuclei part, while the liquid molecular potential energy changes greatly at the beginning of the cavitation nuclei growth. The density of the liquid and the surface layer changes more obvious, but density of vapor in the bubble changes inconspicuously. With the growth of cavitation nuclei, the RDF peak intensity increased, the peak width narrowed and the first valley moved inner. When cavitation nuclei initial size reduced, the peak intensity reduced, the corresponding  $r_{bin}$  increased. With the decrease of the initial cavitation nuclei, the system pressure and total energy achieved a balance longer, and correspondingly, they were smaller. In addition, at the beginning of the cavitation nuclei growth, the total energy and system pressure changed greatly.*

**Keywords:** Cavitation nuclei; Molecular dynamics simulation; Lennard-Jones fluid; Cavitation inception; Nucleation

## INTRODUCTION

Cavitation is a complex flowing physical phenomenon in liquid involving multiphase flow, compressibility and exchange of multiple aspects. In the field of ocean engineering, cavitation is widespread, such as propellers, high-speed underwater weapons, and so on[1]. How to reduce and control the occurrence of cavitation and reduce the negative effects of cavitation is an important research direction in the field of ocean engineering. Cavitation is often accompanied by hydrodynamic disturbance, decline of performance, erosion on solid surface, increase of water resistance, pressure fluctuation, vibration, noise, and so on [2,3]. Therefore, it is

extremely important to study the microcosmic mechanism of cavitation.

Cavitation is one of the key research in fluid mechanics, especially the micro cavitation bubble nucleation. In recent years, the research on micro bubble nucleation mainly is focus on theoretical analysis, experimental research and molecular dynamics (MD) simulations. In the latest theoretical analysis, based on the classical nucleation theory, Kyoko[4], who combined experimental study and numerical results, set up a complete equation about the nucleation rate, and revised Thomas coefficient. Besides, he also found that the improved equation and the classical nucleation theory vary several orders on the bubble nucleation parameter. In the process

of cavitation nuclei experimental research, Mørch, combining theoretical and experimental method, discussed tensile strength and bubble nuclei generation[5], and then studied the bubble nuclei nucleation on solid-liquid interface[6], and verified the experimental results. In addition, Anders Andersen[7] made an experimental and theoretical study on cavitation interface, whose results showed that the cavitation nuclei in experiment were smaller than those were calculated.

With the rapid development of MD simulation, a large number of researchers have carried on MD simulations study of bubble nucleation in L-J fluid. For homogeneous nucleation, Kinjo[8], Yasuoka[9] and Wu[10], investigated cavitation nucleation process of the stretched L-J liquids in homogeneous liquid. According to the simulation results, stable bubbles appeared, when the L-J liquid was stretched to a certain extent to cause liquid density being lower than the certain critical value. Then Sekinea[11] and Vladimir[12,13], also studied the bubble nucleation process in L-J fluid by using the same method, and calculated the system bubble nucleation rate. The results showed that the actual bubble nucleation rate was greater than the predicted value of classical nucleation theory, and indicated that the size effect was not considered in the classical nucleation theory. In addition, Raymond analyzed the bubble nucleation in boiling and cavitation[14], and the results showed that the bubble was non-spherical at initial state, and with the growth of the bubble, it gradually became spherical. The most important was that bubble growth process was in accordance with Rayleigh-Plesset equation. Based on the research of homogeneous nucleation in L-J fluid, there have been some results of heterogeneous nucleation simulation[15,17]. Tsuda discussed the difference in bubble nuclei growth rule between one-component liquid and two-component liquid, and the results showed that coalescence of bubble nuclei appeared frequently in one-component liquid than that in two-component liquid, and the bubble nuclei were more stable near the heterogeneous atoms[17]. In the research of nucleation on the metal surface, Kirandid not only study the bubble nuclei nucleation in L-J fluid with hot nanoparticles by using MD simulation, but also described the formation and rupture of the cavity nanobubbles, and at last concluded the thermodynamic parameters of cavitation formation and rupture of different nanoparticles[18]. In recent years, more and more researchers focus on liquid water bubbles nuclei nucleation[19]. Yijin Mao studied nanobubbles generation and collapse in water by using the MD simulation[20]. And then, Mitsuhiro described the bubble surface tension on bubble nuclei nucleation in water, and found that the surface tension formula of the nanobubbles conformed to the Yong-Laplace (Y-L) equation[21].

In summary, although there has been a certain degree of understanding of bubble nuclei nucleation in the current study, the research on the cavitation mechanism and the influencing factors at a molecular level is not perfect enough. So this manuscript studied bubble nuclei nucleation transient characteristics in cavitation inception and analyzed the changing mechanism of cavitation nuclei and the thermodynamic parameters.

## SIMULATION PARAMETERS SETTING

### THE LENNARD-JONES POTENTIAL ENERGY

Because the parameters value are very small in MD simulation, each parameter was converted into dimensionless number to calculate and analyze conveniently. The specific conversion relations were shown in Tab. 1.

Tab. 1. Parameters Dimensionless Relationship[22]

Dimensionless quantity	Transformation relation
Length $L^*$	$L/\sigma$
Number density $\rho^*$	$\rho\sigma^3$
Time $t^*$	$(\epsilon/m\sigma^2)^{1/2}t$
Temperature $T^*$	$k_B T/\epsilon$
Energy $E^*$	$E/\epsilon$
Pressure $p^*$	$p\sigma^3/\epsilon$

L-J fluid was employed as the simulation study object, which might be caused by the reason that structure of L-J fluid is relatively simple, and it is not involved effect of the bond angle and coulomb force. In addition, it is also an important reason that the experimental data is relatively abundant, and the intermolecular forces between the liquid and gas can be described by using it.

The L-J potential energy function  $u_{LJ}$ , which is a function of intermolecular distance  $r$ , is given by[17]

$$u_{LJ}(r) = 4\epsilon \left[ \left( \frac{\sigma}{r} \right)^{12} - \left( \frac{\sigma}{r} \right)^6 \right] \quad (1)$$

where the potential well depth  $\epsilon$  and the characteristic length  $\sigma$  are potential energy parameters. In this manuscript, the potential energy parameters of argon atoms are set as  $\epsilon/k_B = 115.5\text{K}$ ,  $\sigma = 0.3385\text{nm}$ , where  $k_B$  is Boltzmann's constant [17]. In order to reduce the computational cost, the cut-off processing was adopted for the potential energy model in this manuscript, and the simulation was conducted with a cut-off distance  $r_c = 2.5\sigma$ .

Permanent gas bubble nuclei are a necessary condition of the cavitation initial nucleation process in liquids, so the helium is applied as non-condensed gas nuclei, and its potential energy parameters are set as  $\epsilon_s/k_B = 10.2112\text{K}$ ,  $\sigma_s = 0.2556\text{nm}$ . The interaction parameters between two different kinds of molecules,  $\epsilon_{AB}$  and  $\sigma_{AB}$  are obtained by the Lorentz-Berthelot rules[22], that are calculated from

$$\sigma_{AB} = \frac{1}{2} (\sigma + \sigma_s) \quad (2)$$

and

$$\epsilon_{AB} = \sqrt{\epsilon \cdot \epsilon_s} \quad (3)$$

## SIMULATION PARAMETER SETTINGS

The computational domain was filled with 64000 argon atoms in the simulation, which was built with the face-center cubic (FCC) unit of cubic lattice distribution at the initial position. The center of the computational domain was set to be the cavitation nuclei, whose initial size of dimensionless radius  $R^*= 2,5,10$  respectively and its slices of the model were showed in Fig.1. In the simulation process, canonical ensemble (NVT) was adopted in this research, which acquired that number of molecules  $N$ , computational domain volume  $V$  and temperature  $T$  were constants in the computational domain. And in the process of cavitation, temperature can be thought to be constant, while system pressure and total energy would change with cavitation nuclei growth. The influence of pressure change is very important to research cavitation in liquid, so the NVT was used to control the system temperature. Because of inertia in the liquid, generally, the volume and quality of liquid around the cavitation nuclei are considered constant in a very short time, therefore NVT was used to fix system volume in this study. Other conditions were as follows: the initial velocity of each argon atom distribution was a series of random numbers under an absolute temperature in the system, which was in accordance with Maxwell distribution. Periodic boundary conditions were applied in the calculation model, and verlet leap frog method was adopted to calculate Newton equations. The method of interval sampling was used, and simulation steps were 1.0fs. The total time was set to be 1000ps.

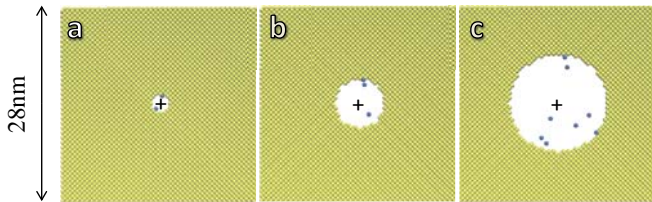


Fig.1. Model section. The section thickness is 0.1nm, where the blue particles gas molecules, and the '+' markers indicate their center-of-masses; a)  $R^*=2$ ; b)  $R^*=5$ ; c)  $R^*=10$

Simultaneously, the temperature control system was introduced in the computational domain to correct the velocity of two kinds of molecules, which ensured a constant temperature. Here, the temperature and pressure are calculated from[17]

$$T = \frac{2}{3Nk_B} \sum_i \frac{1}{2} m v_i^2 \quad (4)$$

and

$$p = \rho k_B T - \frac{1}{3V} \sum_{i<j} \sum_j r_{ij} \frac{\partial u_{JJj}}{\partial r_{ij}} \quad (5)$$

where  $m$  is the molecular mass,  $\rho$  is density,  $N$  is the total number of molecules in the computational domain,  $V$  is the

volume of the computational domain,  $v_i$  is the speed of atom No. $i$ ,  $k_B$  is the Boltzmann's constant,  $u_{JJ}$  is the potential energy function, and  $i$  and  $j$  is different molecules number.

In order to accurately obtain the transient characteristics of cavitation nucleation, molecular structure was set to be stable before the calculation, so relaxation time and energy minimization method was carried out. In the relaxation time, the temperature and pressure were key to characteristic parameters whether the system was stable. The total steps of relaxation time were set to be 5000ps.

The change of the system temperature and pressure was shown in Fig.2 with the dimensionless number density  $\rho^*=0.5924$  at the temperature  $T=84K$ . From the temperature curve (see Fig.2(a)), the system temperature reached equilibrium stage (III) after 1200ps, so the computational domain was regarded as reaching equilibrium before the liquid argon overheated. The eventual equilibrium temperature value was almost a constant, which fluctuated at about 84.05K. From the pressure curve (see Fig.2(b)), The pressure tended to be balanced and at equilibrium stage (III). And the balanced pressure was not over 0MPa at equilibrium stage (III), which caused the system was in a tension state to guarantee the existence of cavitation nuclei. When cavitation nucleus appeared in liquid, the greater the cavitation nuclei were, the greater the pressure increase was, but finally the pressure equilibrium value was consistent with the others.

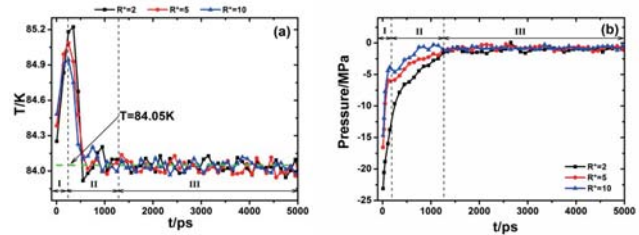


Fig.2. The system temperature (a) and pressure (b) change in relaxation process. I) initial stage; II) transition stage; III) equilibrium stage.

## SIMULATION RESULTS AND ANALYSIS

### CAVITATION NUCLEI EVOLUTION PROCESS

In cavitation inception, the mass and volume of the liquid around cavitation nuclei can be regarded as the constant in a very short time, which caused by the inertia of the liquid mass, accordingly the sampling and calculation of the liquid region with cavitation nuclei was carried out. When the saturation pressure of liquid argon reached overheated state, the growth of cavitation nucleus was shown in Fig. 3 under the NVT ensemble with a stable volume and temperature.



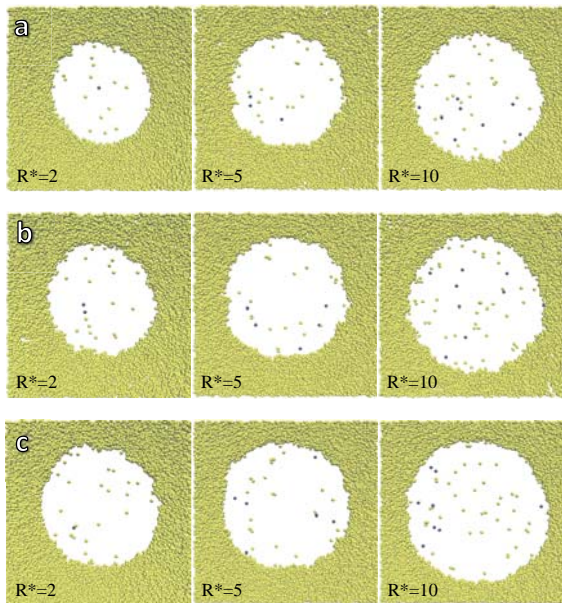


Fig.3. Time evolution of cavitation nuclei section. The section thickness was 0.1nm; a)  $t=10ps$ ; b)  $t=100ps$ ; c)  $t=1000p$

From Fig.3, the radius of cavitation nuclei increased gradually with time, and the growth process of cavitation nucleus with different initial size was similar. Because the liquid and the vapor of argon molecules did not reach equilibrium state in the system, the change of argon molecules from liquid into cavitation nuclei occurred continuously with decreasing pressure at the beginning of the growth, and the cavitation nuclei radius would increase constantly to reach a certain value eventually. Owing to the restriction of computational domain, the cavitation nuclei could not increase infinitely. So the cavitation nuclei changed faintly at the later growth, which indicated the vapor and liquid reached dynamic equilibrium. The shape of cavitation nucleus tended to be spherical over time because of the intermolecular forces, and molecules was gather together by the intermolecular forces, which was the surface tension on the macro level. Therefore in the cavitation nuclei growth process, the shape of the cavitation nucleus was always spherical.

In Fig.3, the larger the cavitation nucleus initial size was, the larger the cavitation nuclei final size was. It was for the reason that the cavity volume and permanent gas molecules number were larger because of the larger cavitation nuclei initial size, which caused the frequent interaction increased between gas molecules and liquid molecules, and the activity enhancement of liquid molecular in the surface layer was carried out. That is to say, under the same condition, the probability for argon atoms entering the cavitation nuclei increased, so the final cavitation nuclei would be larger. The distribution in surface layer of cavitation nuclei was unsmooth, and uneven, which proved that surface layer molecules into the cavitation nuclei were not consistent. It was likely that the interfacial vaporization heat of one molecule in the surface layer was carried out, which led to potential energy of other molecules around it reducing, and activity

decreased. In addition, the probability for other molecules from the surface layer into cavitation nuclei decreased.

From Fig.3, it can be seen that there were cavitation nuclei containing permanent gas in liquid during the cavitation inception. Because of the liquid local pressure decreasing, the enhancement of the molecular activity was carried out in the surface layer, which caused the liquid molecules entered the cavitation nuclei continuously because of its vaporization, and the vapor molecules constantly condensed into liquid molecules. But the number of evaporative molecules was more than that the vapor molecules condensing into the liquid, which contributed to the growth of the cavitation nuclei. With the liquid molecules entering the cavity, the cavitation nuclei would constantly be expand, but their size wouldn't change dramatically because of the computational domain limitation, when the cavitation nuclei grew to a certain size. If the computational domain was large enough, the cavitation nuclei would become bubbles which continuously developed and eventually formed the cavitation on the macro level.

## THERMODYNAMIC PARAMETERS CHANGE OF CAVITATION NUCLEI GROWTH

### THE MOLECULAR POTENTIAL ENERGY CHANGE IN THE COMPUTATIONAL DOMAIN

Molecular potential energy was a key parameter to the stability of molecular structure, and it was one of the important indexes to distinguish vapor. So the molecular potential energy was analyzed and calculated with different time steps in this manuscript.

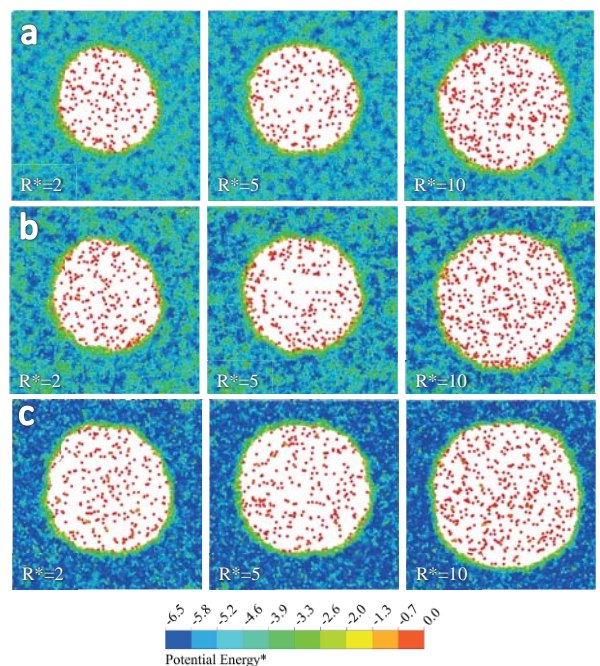


Fig.4. Molecular potential energy change section of cavitation nuclei growth. The section thickness was 0.1nm; a)  $t=10ps$ ; b)  $t=100ps$ ; c)  $t=1000ps$

It was showed that the molecular potential energy variation of cavitation nucleus growth in Fig.4, and it can be seen that molecular potential energy was corresponding to cavitation nuclei evolution in cavitation inception. Comparing Figs. 3 with 4, we could see that the vapor potential energy increased gradually, which mainly caused by the liquid molecules continually entered the vapor region, resulting in a constant growth of cavitation nuclei. From the Boltzmann density distribution law, the vapor number density would decrease with the increase of the potential energy in conservative field, thus the potential energy in cavitation nuclei was considerably higher than that in other region. So, the position, the growth speed, the size and the shape change of cavitation nuclei would be judged according to the potential energy inside the liquid argon. Potential energy of surface layer was higher than liquid but lower than vapor significantly, which meant that the number density of the surface layer larger than liquid but smaller than vapor (verified in Fig.5). In addition, the average intermolecular distance in the surface layer was larger than liquid but smaller than vapor (validated in Fig.7). Since the attraction was greater than repulsion between adjacent molecules in the surface layer. Namely, net tangential attraction was existed in adjacent molecules in the surface layer, which was surface tension source.

From Fig.4, it can be found that the liquid potential energy in the computational domain decreased on the whole, while the potential energy in cavitation nuclei changed faintly with time going by. During the decrease of the liquid potential energy, the reducing speed of different radius was different: before  $t=100\text{ps}$ , the blue region changed least with  $R^*=2$ , but mostly with  $R^*=10$ . Therefore in cavitation nuclei growth, the decrease amplitude of liquid potential energy was different with various cavitation nuclei. So the larger the cavitation nuclei initial size was, the greater the reduction of liquid potential energy was at the same time. It was because the gravitational potential energy on the surface layer was proportional to the surface area, that is, the larger the initial size was, the larger the surface area was, which caused that potential energy of surface layer molecular was greater and molecular structure of the surface layer was more unstable. It meant that the molecular activity enhancement in the surface layer was carried out, which increased the probability of entering the cavity, resulting in the molecular potential energy reducing faster. There were some molecules with stronger activity in the surface layer because of high molecular potential energy, so the potential energy of the surrounding molecules must be lower, and its structure was more stable. Therefore, it verifies the surface layer was rough and coarse in the aspect of the potential energy.

With time going by, the molecular potential energy gradient between vapor and liquid tended to be concentrated, and the surface molecules were in an unbalanced state. Besides, the potential energy gradient changed greatly because of the effect of attraction. For different initial size of cavitation nuclei in the liquid, the variation of potential energy inside the surface layer was similar. This was because that although the cavitation nuclei surface were different, the radius of

curvature were similar, which contributed to a similar change of the molecular potential energy. Under the isothermal condition, the surface free energy was the sum of all molecules gravitational potential energy, so, the surface free energy had a tendency to decrease because of potential energy decreasing. Thus a shrinking tendency was carried out in surface layer, which showed why the bubbles were spherical from another aspect, and it was also the reason for a consistent surface potential energy distribution of cavitation nuclei.

To sum up, at the beginning of the cavitation nuclei growth, the molecular potential energy was larger and the molecular activity was stronger in the liquid and surface layer, in addition, the molecular internal structure stability was poorer, which caused that the liquid molecules escaped attraction of surrounding molecules to enter the vapor. With the cavitation nuclei growing, liquid density increased in a short time, thus causing that the molecular structure tended to be stable, which was characterized by the reduction of the liquid molecular potential energy.

### COMPUTATIONAL DOMAIN DENSITY CHANGE IN THE CALCULATION DOMAIN IN CAVITATION INCEPTION

In order to have a closer look at the density variation, the spatial density profile was computed by averaging density in bubble center and radially bin which are built by uniformly chopping the simulation box in the horizontal direction; the final profile of density are shown in Fig. 5.

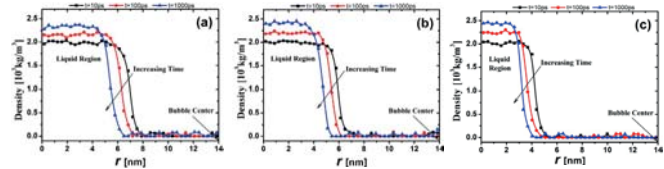


Fig.5. Computational domain density variation. a)  $R^*=2$ ; b)  $R^*=5$ ; c)  $R^*=10$

From the density variation curves in Fig.5, with different initial size, the density curves variation was similar. It can be seen that liquid density kept increasing with liquid volume decreasing and the density of vapor in the bubble was constant, despite vapor volume increasing with time going by. The density variation of the surface layer was sharper, and its severity variation did not change with time. In cavitation inception, the density of liquid region surrounding cavitation nuclei was increasing in a short time, and corresponding to Fig.4. The greater the liquid density, the smaller the potential energy, which caused the molecular structure was more stable. The surface layer density was between the liquid and vapor, thus its potential energy was somewhere in between, which also confirmed indirectly that the Boltzmann distribution law was applicable even to the molecular level.

From 3 pictures in Fig.5, the smaller the initial size of cavitation nuclei, the longer the interval of the density variation curve in the surface layer, so the cavitation nuclei growing space here was bigger. While the liquid region was



on the contrary, the density curve interval was longer with the larger initial size of cavitation nuclei. The main reason was that the cavitation nuclei became larger with the smaller liquid region. But the inertia of liquid was still existed, so the density here became denser and the potential energy became smaller in a short time. That is to say if the initial size of cavitation nuclei was larger at first, then the liquid region density was larger in the final growth of cavitation nuclei. In addition, the potential energy here was smaller and the structure of liquid molecule around cavitation nuclei was more stable, but the growing space of cavitation nuclei was smaller. In Fig.5(c), the curve interval in the position of surface layer between  $t=10\text{ps}$  and  $t=100\text{ps}$  was wider than that between  $t=100\text{ps}$  and  $t=1000\text{ps}$ , which showed that the growth rate here was reduced significantly in the latter of the simulation, when the cavitation nuclei initial size was  $R^*=10$ . Although the distance in the other two figures curves was not wide compared to the former, the growth of the other two kinds of cavitation nuclei was declined to some extent, since the time scale between the 2 curves was 10 times.

Thus, in cavitation inception, because the cavitation initial stage was very short, there was a time lag of the liquid surrounding cavitation nuclei moving, so the density variation of the liquid and the surface layer was more obvious, and the density of vapor in the bubble was constant.

#### THE CAVITATION NUCLEI DIAMETER CHANGES IN CAVITATION INCEPTION

In cavitation inception, the cavitation nuclei size change was the focus of researchers all the time, and the size change of the cavitation nuclei determined whether cavitation bubbles could be produced, so this manuscript monitored and analyzed the cavitation nuclei transient changes in cavitation inception.

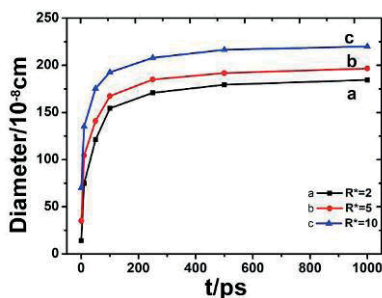


Fig.6. Cavitation nuclei diameter changes

Fig.6 showed the changing curve for cavitation nuclei diameter, and the three curves respectively represented the growth of different initial cavitation nuclei, which could be seen from the figure that the cavitation nuclei diameter had obvious changes. Before  $t=200\text{ps}$ , the three growth curves increased more sharply, but the curves increase reduced rapidly because of the limitation of the computational domain, which was consistent with the density variation (Fig.5), when time was between  $200\text{ps}$  and  $1000\text{ps}$ . There

was a certain difference among the three curves in the figure, since the cavitation nuclei final diameter depended on its initial radius, which caused that the larger the initial radius was, the greater the final diameter was. During the cavitation nuclei growth, under the same condition, the growth speed was relatively rapid if the initial radius of cavitation nuclei was large, on the contrary its growth was relatively slow if the initial radius was small.

Tab. 2. Cavitation nuclei diameter change

Type	$R^*=2$	$R^*=5$	$R^*=10$
Initial diameter $D_0$	14.016	35.04	70.08
Maximum diameter $D_{\max}$	184.537	189.586	219.998
Growth rate = $(D_{\max} - D_0)/D_0$	12.2857	4.2561	2.1514

As can be seen from table 2, the growth rate of  $R^*=2, 5$  and  $10$  was  $12.2857, 4.2561$  and  $2.1514$ , respectively. By contrast, it can be found that the growth space of cavitation nuclei was larger if its initial radius was smaller, but its final size was smaller than that of the cavitation nuclei with larger initial diameter. It showed that under the same external conditions, the smaller cavitation nuclei growth was same as the larger cavitation nuclei, but its growth needed a long time. With computational domain permitting, the cavitation nuclei surface area was greater, which caused the high resistance appeared, so the growth space of cavitation nuclei became smaller.

The rapid growth of cavitation nuclei was occurred so that cavitation nuclei grew into bubbles rapidly (calculation domain permitting) in cavitation inception, which confirmed a „sudden” cavitation inception rather than a „calm” one. Cavitation nuclei diameter was necessary to the cavitation on the micro level, and the larger the initial radius was, the faster its growth rate was.

#### THE MOLECULES RADIAL DISTRIBUTION FUNCTION (RDF) IN CAVITATION INCEPTION

The internal structure change of liquid was very important in the cavitation process, so this manuscript analyzed it by combining the RDF.

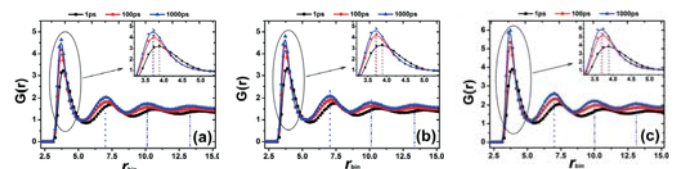


Fig.7. The changes of molecular RDF. a)  $R^*=2$ ; b)  $R^*=5$ ; c)  $R^*=10$ ;  $r_{\text{bin}}$  was the intermolecular distance

The RDF changes of liquid argon molecules were shown in Fig.7.(a), (b) and (c), which showed that the RDF was 0 when  $r_{\text{bin}} < 3.21\text{\AA}$ , that is, the recent distance between adjacent molecules would not be less than  $3.21\text{\AA}$ . When  $r_{\text{bin}} = 3.9\text{\AA}$ ,  $G(r)$  has reached the first peak, and this time,  $r_{\text{bin}}$  represented

the most likely distance of two adjacent liquid molecules in the cavitation nuclei growth, where the here  $r_{bin}$  was lowest point of the intermolecular interaction potential. As  $r_{bin}=7.25\text{\AA}$ ,  $G(r)$  reached the second peak which was the liquid molecules second shell peak, and at this time  $r_{bin}$  was corresponding to the distance between the center liquid molecule and that of the second shell. And the third peak appeared at about  $r_{bin}=10.9\text{\AA}$ , and the peak intensity gradually weakened. In addition, all the RDF tended to be a stable value when  $r_{bin}>14.3\text{\AA}$ , that is, when the distance exceeded  $14.3\text{\AA}$ , the system molecules were similar to the uniform liquid. The above features reflecting the liquid had a short-range in order, long-range out of order. From (a), (b) and (c) in Fig.7, it can be found that in the entire growth of cavitation nuclei, the liquid RDF had several peaks, which represented the first coordination sphere, the second coordination sphere, et al respectively of the center molecule, and the peaks attenuated quickly with time going by. So it can be concluded that the orderly arrangement of liquid molecules disappeared with the increase of the intermolecular distance. And also, it can be said that the areal density, on average, was greater than the average density near the peak position. Although the cavitation nuclei initial size was different, the curve of RDF was roughly the same, that it, for the first peak, before  $t=100\text{ps}$  and with time going by, the peak intensity of the RDF increased gradually, while the peak width narrowed gradually. When  $t>100\text{ps}$ , the two curves interval in the first peak became smaller, which indicated that the peak intensity and the peak width achieved a balance. This suggested that when  $t<100\text{ps}$ , at the maximal peak, the probability of liquid molecules appearance would increase with the extension of time. In addition, the density became bigger gradually, which caused that the molecular distribution was loose and out of order, and the internal structure stability was poor, that the vaporization of liquid molecules was serious. With the growth of cavitation nuclei, the peak intensity increased, the peak width narrowed and the first valley moved inner. The reason why the above features occurred were that the liquid molecular arrangement at the first coordination sphere became close, the molecular distribution became regularly and the internal liquid structure was stable, which led to the result that the vaporization of liquid molecules decreased gradually. By comparison from the former two peaks, the peak intensity of the second peak became larger with the increasing of cavitation nuclei initial size, while the change of peak width was not obvious, but the width was larger than the former one. The main reason was that the size of cavitation nuclei increased gradually with time going by, which made the volume of liquid region become smaller, the density become heavier and the performance of the peak intensity increase. With intermolecular distance of the second shell  $r_{bin}$  increasing, the molecular disorder became larger and the structure became more unstable, which was accord with the rules that short-range in order, and long-range out of order. Therefore, the performance of the second peak width in RDF did not change with time going by, but it was greater than the first peak width. For the two peaks in RDF, intermolecular

distance  $r_{bin}$  increased with cavitation nuclei initial size decreasing, which could get the following conclusion, with the increasing of pressure in cavitation nuclei, the distance between the liquid molecules were compressed to a certain degree, so the performance of intermolecular distance  $r_{bin}$  decreased in RDF.

Through the partial enlarged graphs in Fig. 7 (a), (b) and (c), by contrast, it can be found that the larger the cavitation nuclei initial size was, the greater the peak intensity of the RDF was, and the most important was that the increase amplitude of the peak intensity was similar. Moreover, the peak intensity of RDF was more different with the greater difference of cavitation nuclei initial size. The change trend of  $r_{bin}$  was contrary to the change of peak intensity: with the extension of time, the position of peak appearance was getting smaller, that the intermolecular distance of liquid was getting smaller, which proved that the liquid pressure was increasing gradually. When  $t=100\text{ps}$ ,  $r_{bin}$  reached an equilibrium value, and it showed the intermolecular distance achieved a balance, which caused the liquid pressure was maintained in stable. The liquid intermolecular distance  $r_{bin}$  would decrease with the increase of the initial size, so the relative liquid pressure also enhanced. In Fig.7, (a), (b) and (c), the position of other peaks occurrence decreased with cavitation nuclei size increasing, but the peak intensity increased as cavitation nuclei size increased. The most obvious was that the greater the initial cavitation nuclei size was, the severer curves amplitude was. Through the analysis of the RDF, it can be concluded that the liquid molecular distribution of RDF was similar to the change rule of the liquid molecular potential energy. At the beginning of the cavitation nuclei growth, the vaporization of liquid molecules was rapid with its liquid volume decreasing, which, under the limit of the computational domain, caused the gradual increase of density, and stability of molecular structure. After that the cavitation nuclei size grew slowly, and the liquid volume and density changed faintly.

Therefore, in cavitation nuclei growth, the molecular distribution inside the liquid became orderly gradually and the liquid density changed over time. And the change of liquid peak has confirmed short-range in order, long-range out of order. At the early growth of cavitation nuclei, the vaporization of liquid molecules was relatively serious and intermolecular distance was greater. While in the later growth, the liquid molecular distribution was relatively regular and ordered with intermolecular distance decreasing to a balance. The peak of the RDF was greater with the larger initial size of cavitation nuclei, so the molecular distribution rule was more regular, which caused relative increase of pressure liquid.

## THE SYSTEM PRESSURE AND TOTAL ENERGY VARIATION IN CAVITATION NUCLEI GENERATION

On the macro level, the occurrence of cavitation was because of the reduction of the external pressure, so it was a necessary condition for cavitation that the system pressure being lower than the saturated vapor pressure. So this

manuscript monitored the pressure of cavitation occurrence in the computational domain.

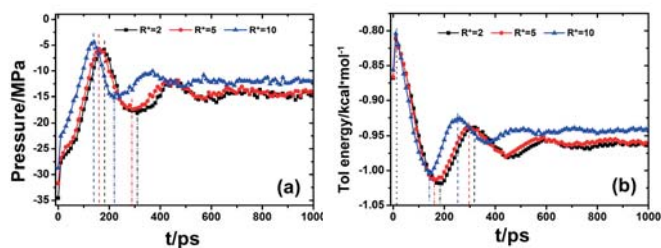


Fig.8. The system pressure (a) and the total energy (b) variation of cavitation nuclei growth.

The three curves in Fig.8 represented the system pressure variation of cavitation nuclei growth. It can be seen that, the system pressure was negative in the entire growth process, which indicated that the liquid region and the growth of cavitation nuclei was in a tension state in the whole computational domain. The absolute value of pressure system was getting maximum, which meant that the entire system was in the maximum tensile force at the initial state of cavitation nuclei growth. Before  $t = 100$  ps, the absolute value of system pressure reduced continuously, which meant that tensile force been in system was reduced gradually. However, cavitation nuclei were in rapid growth at the initial state of cavitation nuclei growth, which might lie in that the average tensile force was larger. When  $100 \text{ ps} < t < 680 \text{ ps}$ , the system pressure has been in fluctuation, and the tensile force was changing constantly, but not affect cavitation nuclei growth with its growth rate decreasing. After  $t = 680$  ps, the system pressure value reached a relatively balanced state, which indicated that the tensile force remained stable and cavitation nuclei growth was maintained at moderate speed. Therefore, the cavitation nuclei grew steadily, and finally became bubbles within the permission of the computational domain after  $t = 680$  ps. The above features meant that before  $t = 100$  ps, the liquid molecules were not stable, which might be attributed to the high potential energy. So it was easier that molecules from the surface layer into the cavitation nuclei, which caused the needed tensile strength decreased gradually. When  $100 \text{ ps} < t < 680 \text{ ps}$ , the liquid internal structure was stable, which might result from that liquid potential energy decreased, so the acquired tensile force increased gradually. But, the system pressure fluctuation was larger, which might lie in that it was a transition state. After  $t = 680$  ps, the potential energy stability was achieved, and the liquid internal structure was more stable, which caused that the tensile force been in cavitation nuclei growth tended to be stable.

In the Fig.8 (a), the overall trend had no difference when  $R^* = 2, 5$  and  $10$ , but it can be seen from the local pressure variation that the absolute value of system pressure was smaller, and the emergence of valley value was shorter, which might lie in that the initial size was greater. As the cavitation nuclei initial size decreased, the emergence of the valley value would be later, and their absolute value would be smaller. Moreover, the pressure balance would also be later in the

meantime. When the cavitation nuclei growth was stable, the absolute value of the system pressure would decrease with the increase of the initial size: The average pressure of  $R^* = 5$  was  $0.8 \text{ Mpa}$  lower than that of  $R^* = 2$ ,  $14.95 \text{ Mpa}$ , while the average pressure of  $R^* = 10$  was  $12.35 \text{ Mpa}$ , which reduced  $1.8 \text{ Mpa}$  compared with  $R^* = 5$ , and the reduction amplitude increased  $55.56\%$ . This was mainly because the cavity in liquid was greater with the larger cavitation nuclei initial size, which jointly caused that tensile force needed for the cavitation nuclei growth became smaller, so the system pressure needed for phases change was smaller. It means that the cavitation occurrence was easier with the larger initial cavitation nuclei size, during external pressure reduced to a lesser extent, under the same external conditions.

Fig.8 (b) was the curve variation of the total energy with the changing of time. From Fig.8 (a) and (b), the total change trend of the system total energy was similar to the system pressure change. Before  $t = 100$  ps, the overall trend reduced gradually. Moreover the total energy has been fluctuant with  $100 \text{ ps} < t < 680 \text{ ps}$ , and after  $t = 680$  ps, the total energy value reached a relatively balanced state.

From the three curves in Fig.8 (b), the total energy firstly reached the maximum value before  $t = 150$  ps, which was around  $1.0186 \text{ kcal/mol}$ . As the cavitation nuclei initial size decreased, the minimum value that the total energy achieved in the initial stage decreased gradually. And when  $R^* = 2$ , the total energy had the least minimum value which was about  $0.975 \text{ kcal/mol}$ . As the difference of cavitation nuclei initial size became smaller, the difference of the minimum value would also be smaller like the first valley value of  $R^* = 2, 5$ . This showed that when the cavitation nuclei appeared in the liquid, the total energy in the initial state has a decreasing process. And with the decrease of the initial cavitation nuclei size, the total energy decreasing process had a downward trend but it had a violent fluctuation before it achieved a balance.

From the Fig.8, it was almost same that the time for the total energy and pressure of the system achieving the best value. It can be seen that with the increase of the initial size, the occurrence time of the first peak reduced, the peak value also increased gradually, and the balanced time for the total energy was shorter. When  $t = 680$  ps, the total energy achieved a balance which became larger with the increase of cavitation nuclei initial size. The total energy of  $R^* = 5$  was  $0.007 \text{ kcal/mol}$  larger than that of  $R^* = 2$ ,  $-0.965 \text{ kcal/mol}$ , while it increased to  $-0.9404 \text{ kcal/mol}$  when  $R^* = 10$ , which increased  $0.0176 \text{ kcal/mol}$  compared with  $R^* = 5$ , and increasing extent increased by  $60.23\%$ .

Compared Fig.8 (a) with (b), it can be found that when there were cavitation nuclei inside the liquid argon, the changing trends of the system pressure and the total energy were similar, which would fluctuate before achieving a balance. As well as, the balance time for the system pressure and total energy would be shorter with the larger cavitation nuclei initial size. At the early stage of the cavitation nuclei growth, the pressure and total energy changed greatly, and they would be much more stable in the middle and the later period of the growth. This meant that, in cavitation inception,



the intermolecular structure in liquid was not stable, which would show a pressure and total energy fluctuation on the macro level. At the later growth stage, the intermolecular structure would be much more stable, which would show a balanced pressure and total energy, at that time, the cavitation nuclei reached a certain value with a stable growth, and finally achieved the cavitation within the permission of the computational domain on the macro level.

## CONCLUSIONS

(1) In cavitation inception of L-J fluid, the larger the cavitation nuclei were, the larger they were finally in the computation domain. Under the influence of the surface tension, the final shape of the cavitation nuclei was spherical.

(2) In the evolution of cavitation nuclei, the potential energy in the vapor region was the highest, and the potential energy in the liquid region was constantly changing. At the beginning of the cavitation nuclei growth, the potential energy in the liquid region decreased with the increase of the cavitation nuclei. The molecular potential energy in vapor was significantly higher than that in the liquid region.

(3) The density of the liquid and the surface layer changes more obvious, but density of vapor in the bubble changes inconspicuously. It was easier for the cavitation nuclei to grow with the larger cavitation nuclei, and under the influence of the computational domain, finally the cavitation nuclei diameter increased first, and then tended to be certain.

(4) With the change of time, the peak intensity of the RDF first peak in liquid region increased gradually, and the peak width narrowed gradually.

(5) In cavitation inception of the L-J fluid, when the cavitation nuclei were growing, the total energy and the system pressure change fluctuated greatly. As the initial cavitation nuclei size decreased, the balance time for the system pressure and the total energy was later, the absolute value of the system pressure was smaller, and the equilibrium value of the total energy was greater.

## ACKNOWLEDGMENTS

This project is partially supported by National Youth Natural Science Foundation of China (51509112), Natural Science Foundation of Jiangsu Province of China (BK20171302), Key R & D programs of Jiangsu Province of China (BE2015129, BE2016160, BE2017140), Prospective joint research project of Jiangsu Province of China (BY2016072-02).

## BIBLIOGRAPHY

1. Zhu, R.S., Chen, Z.L., Wang, X.L., Chao, L.: *Numerical study on cavitation characteristics of CAPI400 nuclear main coolant pump*. Journal of Drainage and Irrigation Machinery Engineering. Vol. 34, no. 6, pp. 490-495, 2016.

2. Knapp, R.T., Daily, J.W., Hammitt, F.G.: *Cavitation*. McGraw-Hill Book Company, New York, 1970.

3. Brennen, C.E.: *Cavitation and Bubble Dynamics*. Oxford University Press, Oxford, 1995.

4. Tanaka, K.K., Tanaka, H., Angéilil, R., Diemand, J.: *Simple improvements to classical bubble nucleation models*. Phys Rev E Stat Nonlin Soft Matter Phys. Vol. 92, no. 2, pp.022401, 2015.

5. Mørch, K. A.: *Cavitation nuclei: experiments and theory*. Journal of Hydrodynamics. Vol. 21, no. 2, pp. 176-189, 2009.

6. Mørch, K. A.: *Cavitation inception from bubble nuclei*. Interface Focus. Vol. 5, no. 5, pp. 20150006, 2015.

7. Andersen, A., Mørch, K. A.: *Cavitation nuclei in water exposed to transient pressures*. Journal of Fluid Mechanics. no. 771, pp. 424-448, 2015.

8. Kinjo, T., Matsumoto, M.: *Cavitation processes and negative pressure*. Fluid Phase Equilibria. Vol. 144, no. 1-2, pp. 343-350, 1998.

9. Yasuoka, K., Matsumoto, M.: *Molecular dynamics of homogeneous nucleation in the vapor phase. I. Lennard-Jones fluid*. Journal of Chemical Physics. Vol. 109, no. 19, pp. 8451-8462, 1998.

10. Wu, Y. W., Chin, P.: *A molecular dynamics simulation of bubble nucleation in homogeneous liquid under heating with constant mean negative pressure*. Nanoscale and Microscale Thermophysical Engineering. Vol. 7, no. 2, pp. 137-151, 2003.

11. Sekine, M., Yasuoka, K., Kinjo, T., Matsumoto, M.: *Liquid-vapor nucleation simulation of Lennard-Jones fluid by molecular dynamics method*. Fluid Dynamics Research. Vol. 40, no. 7, pp. 597-605, 2008.

12. Baidakov, V. G., Bobrov, K. S.: *Spontaneous cavitation in a Lennard-Jones liquid at negative pressures*. Journal of Chemical Physics. Vol. 140, no. 18, pp. 184506, 2014.

13. Baidakov, V. G.: *Spontaneous cavitation in a Lennard-Jones liquid: Molecular dynamics simulation and the van der Waals-Cahn-Hilliard gradient theory*. Journal of Chemical Physics. Vol. 144, no. 7, pp. 074502, 2016.

14. Angéilil, R., Diemand, J., Tanaka, K. K., Tanaka, H.: *Bubble evolution and properties in homogeneous nucleation simulations*. Physical Review E Statistical Nonlinear & Soft Matter Physics. Vol. 90, no. 6, pp. 063301, 2014.

15. Maruyama, S., Kimura, T.: *A Molecular Dynamics Simulation of Bubble Nucleation on Solid Surface*.

Transactions of the Japan Society of Mechanical Engineers  
Part B. Vol. 65, no. 638, pp. 3461-3467, 1999.

16. Tatsuto, K., Shigeo, M.: *Molecular dynamics simulation of heterogeneous nucleation of a liquid droplet on a solid surface*. Nanoscale and Microscale Thermophysical Engineering. Vol. 6, no. 1, pp. 3-13, 2002.
17. Tsuda, S. I., Shu, T., Matsumoto, Y.: *A study on the growth of cavitation bubble nuclei using large-scale molecular dynamics simulations*. Fluid Dynamics Research. Vol. 40, no. 7-8, pp. 606-615, 2008.
18. Sasikumar, K., Keblinski, P.: *Molecular dynamics investigation of nanoscale cavitation dynamics*. Journal of Chemical Physics. Vol. 141, no. 23, pp. 12B648\_1-790, 2014.
19. Yamamoto, T., Ohnishi, S.: *Molecular dynamics study on helium nanobubbles in water*. Physical Chemistry Chemical Physics Pccp. Vol. 13, no. 36, pp. 16142, 2011.
20. Mao, Y. J., Zhang, Y. W.: *Nonequilibrium molecular dynamics simulation of nanobubble growth and annihilation in liquid water*. Nanosc Microsc Therm. Vol. 17, no. 2, pp. 79-91, 2013.
21. Matsumoto, M.: *Surface Tension and Stability of a Nanobubble in Water: Molecular Simulation*. Journal of Fluid Science & Technology. Vol. 3, no. 8, pp. 922-929, 2008.
22. Allen, M. P., Tildesley, D. J.: *Computer simulation of liquid*. Oxford: Clarendon Press, 1987.

## CONTACT WITH THE AUTHORS

**Zhao Yuanyuan, Ph.D.**

email: [ujjsfq@sina.com](mailto:ujjsfq@sina.com)

tel.: 008651188780280

National Research Center of Pumps

Jiangsu University

Zhenjiang Jiangsu 212013

**CHINA**